Wrinkling of a sol-gel-derived thin film

S. Joon Kwon,* Jae-Hwan Park, and Jae-Gwan Park
Materials Science and Technology Division, Korea Institute of Science and Technology, P.O. Box 133, Cheongryang, Seoul, 130-650, Korea

(Received 16 June 2004; revised manuscript received 27 August 2004; published 11 January 2005)

We report on the wrinkle formation in a thin film produced by the sol-gel method. Through the relaxation of stress, which results from the removal of the solvent during the drying process, an isotropic wavy pattern is generated in the form of skeletal branches. The patterns have a dominant wavelength satisfying a relationship of three-fourths order of thickness. Densification of the gelated film is enhanced by an increase in the volumetric strain caused by the evaporation of the remaining solvent from the film. The number of skeletal branches and surface roughness increases as the annealing time progresses, without any change in the skeletal wavelength.

DOI: 10.1103/PhysRevE.71.011604 PACS number(s): 68.37.−d, 46.32.+x, 68.60.Wm, 82.70.Gg

Pattern formation in thin films caused by the relaxation of stress is a phenomenon that is frequently encountered both in nature and in technology [1–14]. One of these patterns is a wrinkling, which occurs in the whole film as a result of the relaxation of stress due to various types of instabilities [1,5–14]. These wrinkle patterns, although they have a certain dominant wavelength associated with them, often exhibit isotropic wave patterns [5–9,11–14]. In the case of the bilayer of a polymer layer capped with a thin metal layer, buckling can occur due to the difference in the thermal expansion coefficients between the two layers [5,8,9,13,14]. In the event of the swelling of thin films, blistering surface patterns are formed [11]. While wrinkle formation in thin films has attracted a great deal of attention, few studies have concentrated on the wrinkle formation of sol-gel-derived thin films [4,15].

In the present study, we provide a theoretical basis for the wrinkle formation of sol-gel-derived thin films. The system being considered is a metal oxide layer deposited on a substrate by the sol-gel method. The stress in the system is generated during the drying process, which takes place at a temperature above the boiling point of the solvent. The resultant characteristic wavelength of the isotropic skeletal wavy pattern, λ, is determined to have the minimum system free energy. We also observed an increase in the number of skeletal branches per unit area of the substrate.

The metal oxide sol used in our experiments was zinc oxide (ZnO) sol. The ZnO sol was prepared according to the synthetic method described by Greene *et al.* [17]. The as-obtained sol was spin coated onto a bare silicon (100) substrate to form a 30–400-nm-thick film, and the prepared samples were annealed in a vacuum oven at 150 °C for 0.5–48 h. The wrinkled structure was examined by a scanning electron microscope (SEM, SE-3000, Hitachi) and field emission scanning electron microscope (FESEM, S-4200, Hitachi). The average length of the skeletal branches, the root-mean-square surface roughness, and the skeletal wavelength of the patterns were measured by atomic force microscope (AFM, Dimension 3100, Digital Instruments).

In sol-gel-derived thin films, compressive stress due to the difference in the thermal expansion coefficients between the film and substrate is generated during the drying process, which leads to bending of the gelated thin film. For the isotropic wrinkle, a wave function in one direction with the amplitude ε and the wave number k ($\lambda = 2\pi/k$) can be adapted as shown in Fig. 1(a). The free energy per unit area of the system, which is required to bend the film, is given by [18]

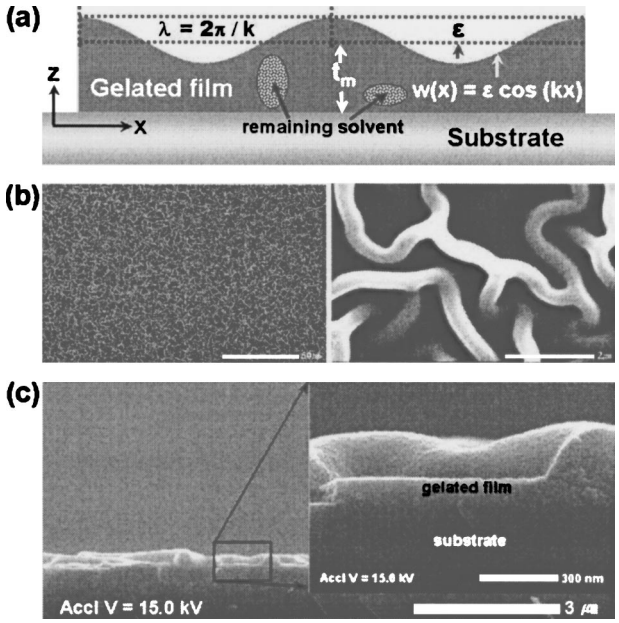

FIG. 1. (a) The geometry of the deformed sol-gel-derived film on a substrate. (b) Plane SEM images showing representative wrinkle patterns in the form of skeletal branches for the ZnO film (film thickness = 85 nm) annealed at 150 °C for 18 h (scale bars are from left: 50 and 2 μm, respectively). (c) A cross-sectional FESEM image of the wrinkle patterns of the film. The inset is a magnified FESEM image of the wrinkled region.

*Author to whom correspondence should be addressed. Electronic address: cheme@kist.re.kr

$$F_b = \left[\frac{E_m t_m^3 k^2}{12(1-\sigma_m^2)} \right] \frac{\varepsilon^2 k^2}{4}, \tag{1}$$

where E_m is the Young's modulus, t_m is the thickness, and σ_m is the Poisson's ratio of the ZnO film. The external strain $\varepsilon^2 k^2/4$ in Eq. (1) is a constant for a relatively small value of $t_m k$ ($t_m k \ll 1$) [8].

As the remaining solvent begins to evaporate during the drying process, the network structure also starts to build up. During this process, the solvent is drawn from the structure since the network exposed to the environment with the larger interface energy given by the solid-vapor interface instead of the solid-liquid interface, and this constitutes a mass transport satisfying Darcy's law, which leads to spontaneous contraction of the network structure [16]. The structure deformation caused by this network contraction is similar to case of the syneresis process in which continuing condensation-reaction-derived spontaneous network shrinkage by expulsion of liquid takes place. The resultant networks usually have an interconnected skeletal branch structure that is attached to the substrate while the solvent is drawn from the interior of the structure to the surface of the structure by the capillary pressure gradient. Therefore, as in the case of thermal stress induced by the difference in the thermal expansion coefficients between the two layers, the drying process gives rise to an internal stress. The internal stress is enough to induce the bending of the gelated thin film; however, it does not cause fracture of the film. And the stress in the gelated film can be written with the effective syneresis stress, as follows [16]:

$$\sigma(z) = \frac{\tau_p E_m}{(1+\sigma_m)} \frac{2V_E}{t_m} \left\{ \frac{\kappa \cosh[\kappa(2z - t_m)/t_m]}{\sinh(\kappa)} \right\},$$

$$\kappa = \sqrt{\frac{\eta(1-2\sigma_m)(1+\sigma_m)}{4\tau_p E_m (1-\sigma_m)}}, \tag{2}$$

where τ_p is the relaxation time for the transition of the film from an elastic state to a viscous state, V_E is the volumetric evaporation rate of the solvent per unit area of the film, and η is the shear viscosity of the gelated body. The internal stress can be considered to have a z orientation in the whole layer as a result of the constraint imposed by the substrate when the syneresis occurs. The syneresis process is brought about when the network of the gelated film is in the viscous state, since no change in the skeletal wavelength of the wrinkles was observed during the drying process in our experiment. The free energy of the drying stress per unit area of the system, F_d, can be calculated in the overall film using Eq. (2) for $\sigma_m = \frac{1}{3}$ as follows:

$$F_d = \frac{1}{\lambda^2} \int_0^{\lambda} dx \int_0^{\lambda} dy \int_0^{t_m} \sigma \, dz = \frac{3\tau_p E_m V_E}{2}. \tag{3}$$

Then, the total free energy of the wrinkled gelated thin film, F_T, can be written as follows:

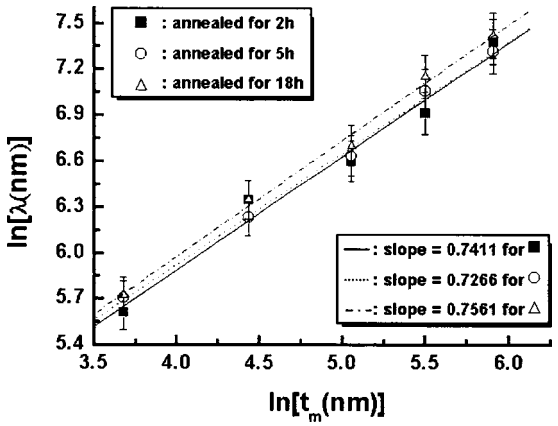

FIG. 2. Comparisons of the theoretical predictions with the different experimental data. Symbols are used to indicate the different experimental data, and the three different lines corresponding to the theoretical results are identified by the slopes referred to in the inset. The dark square symbols, circle, and triangle symbols refer to the wrinkle patterns of the ZnO films (film thickness = 85 nm) annealed at 150 °C, for 2, 5, and 18 h, respectively.

$$F_T = \left(\frac{3E_m t_m^3 k^2}{32} + \frac{6\tau_p E_m V_E}{\varepsilon^2 k^2} \right) \frac{\varepsilon^2 k^2}{4}. \tag{4}$$

From Eq. (4), the dominant wavelength of the skeletal branches, λ, is determined by minimizing the total system free energy with respect to the wave number:

$$\lambda = \pi \left(\frac{\varepsilon^2}{4\tau_p V_E} \right)^{1/4} t_m^{3/4}. \tag{5}$$

The observed values of λ ranged from 270 to 1590 nm as the film thickness increased from 40 to 369 nm. Representative experimental results for the wrinkles are shown in Figs. 1(b) and 1(c). As is apparent from the figures, these wrinkled structures show an isotropic wavy morphology with a distinctive skeletal wavelength over the surface. Comparisons are shown in Fig. 2 between the theoretical values obtained from Eq. (5) and the experimental results for three different annealing times, in which the thickness of the film was varied. The skeletal wavelength of the wrinkles was measured by fast Fourier transformation (FFT) examined by AFM. The plots show a linear relationship between the natural logarithm of λ and the natural logarithm of t_m, giving the value of the slope of the line in the range between 0.727 and 0.756. These values of the slope match well with the predicted value 0.75 obtainable from Eq. (5).

One interesting finding in this study is that the characteristic skeletal wavelength of the wrinkles shows a dependence on the film thickness, such that $\lambda \sim t_m^{3/4}$ rather than $\lambda \sim t_m$, as is usually the case in the context of buckling. Sharp and Jones [11] reported this dependence of the wavelength on the film thickness in the case of the swelling of poly (*d*,*l*-lactide) film on a substrate. While buckling results from the relief of thermomechanical stress, the wrinkle formation in the gelated film corresponds not only to the thermomechanical stress, but also to the drying stress. When the film is heated to a temperature above the boiling point of the solvent, spon-

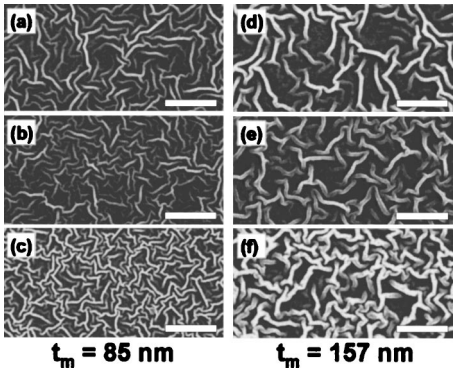

FIG. 3. SEM images of the temporal variation of the skeletal branches of the ZnO film annealed at 150 °C. (a) Wrinkle pattern of 85-nm-thick film annealed for 2 h, (b) annealed for 10 h, (c) annealed for 18 h, and (d) wrinkle pattern of 157-nm-thick film annealed for 2 h, (e) annealed for 10 h, and (f) annealed for 18 h. Scale bars denote 10 μm.

taneous contraction of the interconnected network and associated bending of the film take place. In our experiment, no wrinkles of any kind were observed when the films were annealed at a temperature below the boiling point of the solvent. Therefore, the drawing of the solvent from the film plays a significant role in determining the distinct properties associated with the process of the gelation, such that $\lambda \sim t_m^{3/4}$. Although almost of the solvent evaporates rapidly during spin coating, the remaining solvent evaporates during the drying process, which leads to the creation of a capillary pressure gradient resulting in tension [16]. This induces the development of the stresses in the film, which are needed for the skeletal network contraction. In the case of the wrinkling of a lead titanate film, Sengupta *et al.* [4] reported that the shrinkage of almost 40% of a gelated body that occurs normal to the substrate is due to the loss of the remaining solvent.

In comparing the wrinkle formation of the sol-gel-derived film with that of thin bilayer films of an elastic metal on a viscoelastic polymer, we found some differences in the kind of wrinkling that occurred in these two cases. In the case of the buckling of the bilayer, the annealing temperature is raised above the glass transition temperature of the viscoelastic layer, the layer experiences a transition of elastic to viscoelastic, and the wavelength has a characteristic relation, such that $\lambda = At_m/[B+(C+t_m^3)^{1/2}]^{1/3}$ [8], where A, B, and C are all constants. In the case of the wrinkling of the gelated film, the temperature is raised above the boiling point of the solvent and the film suffers a transition from viscous to viscoelastic. In this case, the film is subjected to a large amount of stress, which gives rise not only to the bending of the film, but also to the contraction of the skeletal network.

One notable finding in this study is the dependence of the number density of skeletal branches on the annealing time. The drawing of the solvent from the film leads to network formation along with continuous contraction. This process induces an increase in the volumetric strain of the gelated body. Although this increase could be achieved by an increase in the skeletal wavelength, in reality the wavelength remains constant and, therefore, no skeletal densification occurs throughout the entire length of the drying process. In Fig. 3, the experimental results show that there is no difference among the skeletal wavelengths of the wrinkles in the samples annealed for different time periods ranging from 2 to 18 h. In other words, the skeletal density does not vary

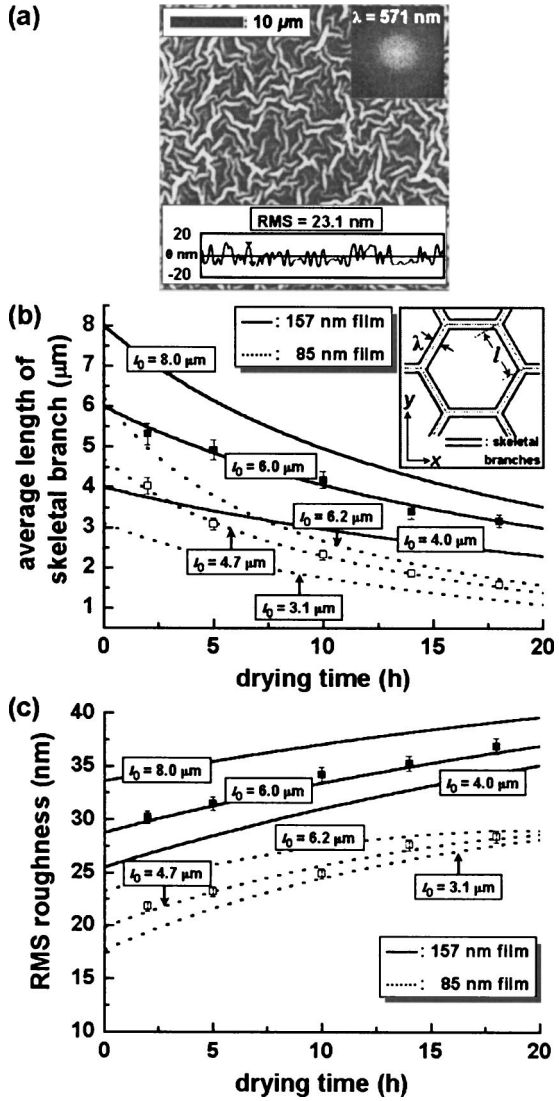

FIG. 4. (a) Plane AFM image of skeletal wrinkles of 85-nm-thick film annealed at 150 °C for 5 h (40 μm × 40 μm). The FFT image for the wrinkles is given in the upper right inset, and the cross-sectional profile is shown in the lower inset. (b) Comparison of the theoretical predictions with the experimental results of the average length of skeletal branches. Solid lines and dotted lines are used for the prediction of the wrinkles in the 157-nm-thick film (average amplitude = 42 nm) and in the 85-nm-thick film (average amplitude = 29 nm), respectively. Dark and open symbols are for the experimental results of the wrinkles in the 157-nm-thick film and in the 85-nm-thick film. The inset is a simplified two-dimensional model of hexagonally interconnected skeletal branches. (c) Comparison between theoretical predictions with experimental results of the rms. The solid and dotted lines represent the predictions, while the dark and open symbols represent the experimental results as in the caption of (b). Volumetric evaporation rate of the solvent per unit area of the film is assumed as 0.1 nm/h.

during the drying process, and the network contraction contributes to the shrinkage of the gelated film until the evaporation of the remaining solvent in the network is completed. As a result, the gelated film density is continuously increases. Therefore, the contraction of the skeletal network should be accompanied by a larger number density of skeletal branches, as is apparent in the experimental results pertaining to the temporal variation of the surface wrinkle patterns shown in Figs. 3(a)–3(c) and 3(d)–3(f). A comparison of the model of the two-dimensional hexagonally interconnected skeletal branches of the gelated films with the experimental results of the average length of the skeletal branches and the surface roughness [refer to Fig. 4(a)] can explain this temporal variation. In the hexagonally interconnected skeletal branches [refer to the inset in Fig. 4(b)], the volumetric strain of the drying film, ξ, can be described as a function of λ and ξ, along with the average length of the skeletal branches, l, as follows:

$$\xi = 1 + \frac{8\sqrt{3}\varepsilon}{3l} - \frac{8\varepsilon\lambda}{3l^2}. \tag{6}$$

The rate of increase of ξ is determined by the relationship of the evaporation rate of the remaining solvent, $d\xi/dt = 2V_E/t_m$ [16], and therefore, the time profile of the value of l can be calculated as follows, with the aid of Eq. (6):

$$l(t) = \frac{2{l_0}^2 t_m \varepsilon + \left[4{l_0}^4 {t_m}^2 \varepsilon^2 - \frac{4\sqrt{3}\lambda {l_0}^2 t_m \varepsilon A(t)}{3} \right]^{1/2}}{A(t)},$$

$$A(t) = \sqrt{3} V_E {l_0}^2 t + 4 l_0 t_m \varepsilon - \frac{4\sqrt{3}\lambda t_m \varepsilon}{3}, \tag{7}$$

where l_0 is the average value of the initial length of the skeletal branches. As is apparent from Eq. (7), the average length of the skeletal branches decreases as the drying time progresses and attains the critical value of l, $l_c = 2\sqrt{3}\lambda/3$, when t is equal to the critical time, as determined by $t_C = (t_m \varepsilon / 3\lambda V_E l_0^2)(\sqrt{3} l_0 - 2\lambda)^2$. Comparisons between the expected and experimental values of $l(t)$ are shown in Fig. 4(b), in which the film thickness is varied. To obtain the experimental values of l, the surface areas of the skeletal wrinkles were measured by AFM. When l_0 has the values of 6 and 4.2 μm, Eq. (7) predicts well the experimental results for the 157- and 85-nm-thick films, respectively. This temporal variation of the skeletal wrinkles can be confirmed by the experimental results of the root-mean-square (rms) value of the surface roughness. The temporal variation of the rms value can be expressed as follows:

$$\mathrm{RMS} = \left\{ \frac{4\sqrt{3}\varepsilon^2\lambda}{3l(t)} \left[2 - \frac{\sqrt{3}\lambda}{3l(t)} \right] \left[1 - \frac{\sqrt{3}\lambda}{3l(t)} \right]^2 \right\}^{1/2}. \tag{8}$$

In Fig. 4(c), the rms–drying-time relationship is shown, along with the theoretical expectations obtained from Eq. (8) and the experimental data. The experimental rms values were measured by AFM. As in the case of Fig. 4(b), the theoretically predicted curves match well with the experimental results, when l_0 is 6 and 4.2 μm, for thicknesses of 157 and 85 nm, respectively. The skeletal densification was not observed during 2 days. If the increase in the number density is due to the cross-linking of the network, larger stresses should lead to rupture or cracking. In our experimental results, however, these kinds of instabilities were not observed and, therefore, the increase in the number density of the skeletal branches could be considered to result from the increase in the volumetric strain during the drying process.

In summary, wrinkle formation in sol-gel-derived thin film gives an isotropic wavy pattern, consisting of skeletal branches with a wavelength satisfying the thickness dependency, $\lambda \sim {t_m}^{3/4}$. This is a distinctive feature of wrinkling of sol-gel-derived thin films, as opposed to that in other types of thin films. The interconnected skeletal network of the film sees an increase in the number density of the skeletal branches as the annealing time progresses, and this can be explained by an increase in the volumetric strain of the gelated film.

Dr. Pil J. Yoo at the Seoul National University is acknowledged for AFM examinations.

[1] J. W. Hutchinson, M. D. Thouless, and E. G. Liniger, Acta Metall. Mater. **40**, 295 (1992); J. W. Hutchinson and Z. Suo, Adv. Appl. Mech. **29**, 63 (1992).
[2] H. Tanaka *et al.*, Phys. Rev. Lett. **68**, 2794 (1992).
[3] G. H. Gunaratne *et al.*, Phys. Rev. Lett. **75**, 3281 (1995).
[4] S. S. Sengupta *et al.*, J. Appl. Phys. **83**, 2291 (1998).
[5] N. Bowden *et al.*, Nature (London) **393**, 146 (1998).
[6] K. Dalnoki-Veress, B. G. Nickel, and J. R. Dutcher, Phys. Rev. Lett. **82**, 1486 (1999).
[7] V. Shenoy and A. Sharma, Phys. Rev. Lett. **86**, 119 (2001).
[8] P. J. Yoo, S. Y. Park, and H. H. Lee, Adv. Mater. (Weinheim, Ger.) **14**, 1383 (2002).
[9] N. Sridhar, D. J. Srolovitz, and Z. Suo, Appl. Phys. Lett. **78**, 2482 (2001).
[10] E. Sharon *et al.*, Nature (London) **419**, 579 (2002).
[11] J. S. Sharp and R. A. L. Jones, Phys. Rev. E **66**, 011801 (2002).
[12] E. Cerda and L. Mahdevan, Phys. Rev. Lett. **90**, 074302 (2003).
[13] P. J. Yoo and H. H. Lee, Phys. Rev. Lett. **91**, 154502 (2003).
[14] S. J. Kwon, P. J. Yoo, and H. H. Lee, Appl. Phys. Lett. **84**, 4487 (2004).
[15] J. T. Dawle *et al.*, J. Mater. Res. **17**, 1900 (2002).
[16] C. J. Brinker and G. W. Scherer, in *Sol-Gel Science: The Physics and Chemistry of Sol-Gel Processing* (Academic, New York, 1990).
[17] L. E. Greene *et al.*, Angew. Chem. **115**, 3139 (2003).
[18] L. D. Landau and E. M. Lifshitz, *Theory of Elasticity*, 3rd ed. (Pergamon, Oxford, 1986).